# Kinetics and Mechanism of Solvolysis of Precocene I 3,4-Oxide: Change in Rate-Determining Step and Trapping of an Intermediate in an Epoxide Solvolysis Reaction

**J. M. Sayer,* S. J. Grossman, K. S. Adusei-Poku, and D. M. Jerina**

*Contribution from the Laboratory of Bioorganic Chemistry, National Institute of Diabetes and Digestive and Kidney Diseases, The National Institutes of Health, Bethesda, Maryland 20892.*
*Received August 31, 1987*

**Abstract:** Solvolysis reactions of most highly reactive benzylic epoxides studied to date exhibit simple biphasic pH–rate profiles consisting of a hydronium ion dependent ($k_H$) and a pH-independent ($k_o$) region. In contrast, the pH–rate profile (extrapolated to zero buffer concentration) for the solvolysis of precocene I 3,4-oxide (3,4-dihydro-3,4-epoxy-7-methoxy-2,2-dimethyl-2*H*-benzo[*b*]pyran) to diols at 25 °C in 1:9 dioxane–water, at ionic strength 0.1 M ($NaClO_4$), is more complex. Besides the transition from $k_H$ to $k_o$ at pH ca. 7, there is a break at pH ca. 9, such that the rate constants observed above this pH fall below those predicted from the pH-independent rate constants determined at lower pH values. Furthermore, the observed rate constants for general acid catalysis of the solvolysis by buffers at pH 8–9.3 show a nonlinear dependence on buffer concentration. Both these observations are consistent with a stepwise mechanism with a change in rate-determining step from formation of a carbocation intermediate (at low pH and low buffer concentrations) to capture of the carbocation by solvent (at higher pH and high buffer concentrations). In the presence of 0.2 M acethydrazide, $CH_3C(O)NHNH_2$, at pH 8.5, approximately 80% of the reaction products corresponded to acethydrazide adducts of the epoxide, although the rate of reaction was increased by less than 10% by the added nucleophile. This is consistent with the trapping of an intermediate subsequent to the rate-determining step. Products of the reaction at low pH are the 3,4-diols resulting from addition of water trans and cis to the epoxide oxygen, whereas at higher pH a substantial fraction (20–75%) of the products corresponds to a ketone produced presumably by a hydride ion shift. On the basis of kinetic and product data, we propose that this ketone is formed from the epoxide by a process that does not share a common intermediate (or pair of intermediates in rapid protonic equilibrium) with the stepwise formation of diols. The kinetic deuterium isotope effect for the migrating hydrogen is estimated to be ca. 4.0.

Precocene I (7-methoxy-2,2-dimethyl-2*H*-benzo[*b*]pyran), a constituent in plants of the *Ageratum* species,[1] induces precocious metamorphosis in insects[2] and is hepatotoxic in rats.[3] The structurally related analogue precocene II (6,7-dimethoxy-2,2-dimethyl-2*H*-benzo[*b*]pyran) has also been shown to be hepatotoxic[4] and nephrotoxic.[5] Enzymatic activation of precocenes I and II to give reactive 3,4-oxides has been proposed as a pathway for the formation of diol metabolites in insects,[6] in rat liver microsomes in vitro[3,4] and in rats in vivo.[7] Through the covalent modification of cellular macromolecules, these oxides are thought to be the agents responsible for the antiallatotropic[8] and hepatotoxic[9] effects of precocene I.

Our interest in the chemistry of the precocene oxides initially arose from their analogy to epoxides that are implicated as ultimate carcinogens metabolically generated from tumorigenic polycyclic aromatic hydrocarbons.[10] A previous study[11] established the extremely high solvolytic reactivity of precocene I 3,4-oxide, **1**,

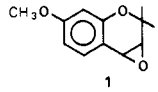

**1**

but contained insufficient kinetic information to permit detailed mechanistic interpretation. Consequently, we have undertaken a more complete kinetic and mechanistic investigation of precocene I 3,4-oxide, under carefully controlled conditions similar to those employed in previous studies[12] of epoxides derived from the polycyclic aromatic hydrocarbons. By analogy with other epoxides[12] we expected to observe a simple biphasic pH vs rate profile at zero buffer concentration, consisting of a hydronium ion dependent and a pH-independent region. However, the pH vs rate profile for the solvolysis of **1** consists of four segments rather than two and exhibits a negative break at pH ca. 9, such that the rate constants observed above this pH fall below those predicted from the pH-independent rate constants determined at pH ca. 7–8.5. In addition, rate constants for catalysis of the solvolysis by buffers show a nonlinear dependence on buffer concentration. We ascribe these observations to a change in rate-limiting step from epoxide ring opening (at low pH and low buffer concentrations) to capture of the resultant carbocation (at higher pH or high buffer concentrations). To our knowledge, this represents the first instance in which such a pH-dependent change in rate-determining step has been observed kinetically in an epoxide solvolysis reaction.

## Results and Discussion

**Effect of pH and Buffer Concentration on Rate.** Figure 1 (lower line and solid symbols) shows the pH dependence of the pseudo-first-order rate constants ($k_{obsd}°$), in the absence of buffer catalysis or extrapolated to zero buffer concentration, for solvolysis of **1** measured at 25 °C and ionic strength 0.1 M ($NaClO_4$) in 1:9 (v/v) dioxane–water. Unlike many epoxide solvolysis reactions,[12] which exhibit simple pH–rate profiles corresponding to a rate law, $k_{obsd}° = k_H a_{H^+} + k_o$, the solvolysis of **1** exhibits a pH–rate profile with a negative break at pH 9–10, such that the observed rate constants at pH values >9 are smaller than those predicted by extrapolation of the line corresponding to the pH-independent rate constants observed at pH 7–8.5. The difference

(1) Kasturi, T. R.; Manithomas, T. *Indian J. Chem.* **1967**, *11*, 91–95.
(2) Bowers, W. S.; Ohta, T.; Cleere, J. S.; Marsella, P. A. *Science (Washington, D.C.)* **1976**, *193*, 542–547.
(3) Halpin, R. A.; Vyas, K. P.; El-Naggar, S. F.; Jerina, D. M. *Chem.-Biol. Interact.* **1984**, *48*, 297–315.
(4) Hsia, M. T. S.; Grossman, S.; Schrankel, K. R. *Chem.-Biol. Interact.* **1981**, *37*, 265–277.
(5) Schrankel, K. R.; Grossman, S. J.; Hsia, M. T. S. *Toxicol. Lett.* **1982**, *12*, 95–100.
(6) Burt, M. E.; Kuhr, R. J.; Bowers, W. S. *Pestic. Biochem. Physiol.* **1978**, *9*, 300–303.
(7) Grossman, S. J.; Hsia, M. T. S. *Toxicology* **1982**, *25*, 293–298.
(8) Pratt, G. E.; Jennings, R. C.; Hamnett, A. F.; Brooks, G. T. *Nature (London)* **1980**, *284*, 320–323.
(9) Ravindranath, V.; Boyd, M. R.; Jerina, D. M. *Biochem. Pharmacol.* **1987**, *36*, 441–446.
(10) Jerina, D. M.; Sayer, J. M.; Agarwal, S. K.; Yagi, H.; Levin, W.; Wood, A. W.; Conney, A. H.; Pruess-Schwartz, D.; Baird, W. M.; Pigott, M. A.; Dipple, A. In *Biological Reactive Intermediates III*; Kocsis, J. J., Jollow, D. J., Witmer, C. M., Nelson, J. O., Snyder, R., Eds.; Plenum: New York, 1986; pp 11–30.
(11) Hamnett, A. F.; Ottridge, A. P.; Pratt, G. E.; Jennings, R. C.; Stott, K. M. *Pestic. Sci.* **1981**, *12*, 245–254.
(12) Whalen, D. L.; Montemarano, J. A.; Thakker, D. R.; Yagi, H.; Jerina, D. M. *J. Am. Chem. Soc.* **1977**, *99*, 5522–5524. Sayer, J. M.; Whalen, D. L.; Friedman, S. L.; Paik, A.; Yagi, H.; Vyas, K. P.; Jerina, D. M. *Ibid.* **1984**, *106*, 226–233. Yagi, H.; Sayer, J. M.; Thakker, D. R.; Levin, W.; Jerina, D. M. *Ibid.* **1987**, *109*, 838–846.

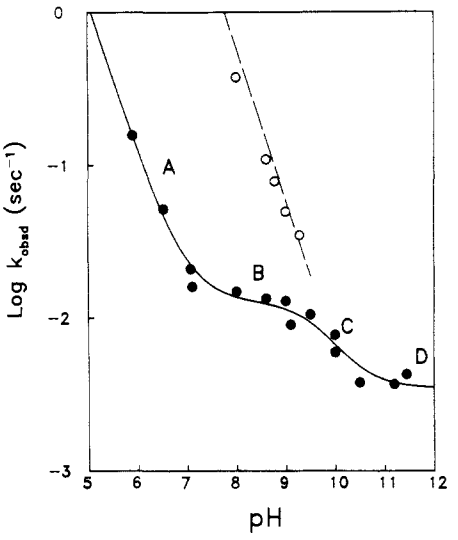


**Figure 1.** Dependence on pH of the observed pseudo-first-order rate constants ($k_{obsd}°$, solid symbols) for solvolysis of **1**, measured in 1 mM buffers (pH ≥10.5), or obtained by extrapolation to zero buffer of data obtained at several low buffer concentrations (pH <10.5). The point at pH 5.9 was determined in the absence of any buffer. In several cases, results of two experiments at the same pH are indicated. For further details of the experimental conditions, see text. The lower curve is calculated from eq 6 and the kinetic constants of Table II. Open symbols represent limiting values for the buffer-independent rate constants ($k_\infty$) at high buffer concentrations (cf. eq 2).

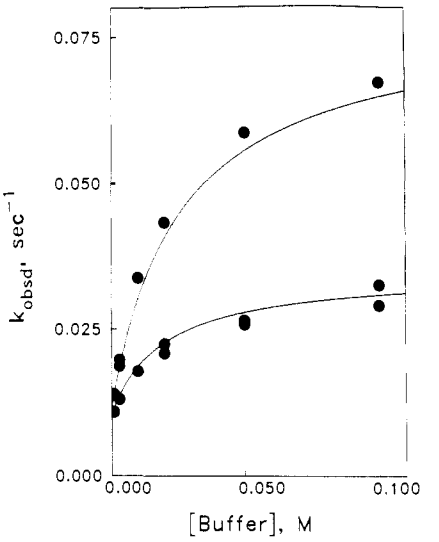


**Figure 2.** Dependence of the observed pseudo-first-order rate constants for solvolysis of **1** on CHES buffer concentration at pH 8.78 (upper curve) and 9.28 (lower curve). The curves shown are based on eq 2, with $k_{st} = k_{obsd} - k_r$ and correspond to $k_{HB} = 4.4$ M$^{-1}$ s$^{-1}$ (Table I) with $k_\infty = 0.079$ and 0.035 s$^{-1}$ at pH 8.78 and 9.28, respectively (cf. Figure 1, open symbols).

in rate for the two pH-independent segments B and D of the pH–rate profile is approximately threefold.

A similar break in the pH–rate profile for phenanthrene 9,10-oxide solvolysis in the presence of 1.0 M potassium chloride, originally ascribed to a change in rate-determining step from ring opening to trapping or rearrangement of the resulting carbocation,[13] was subsequently shown to result from nucleophilic attack upon the epoxide by chloride ion,[14] a process that is kinetically significant only at pH 6–9. A number of other epoxide solvolysis reactions exhibit mechanistically similar pH-dependent acceleration in the presence of halide salts added to maintain constant ionic strength.[15-18] In the present case, this type of mechanism appeared unlikely, since the electrolyte used for control of the ionic strength was sodium perchlorate, which generally does not act as a nucleophile toward epoxides under conditions similar to ours. That nucleophilic attack on the epoxide by perchlorate ion cannot explain the present results was verified by measurement of the rates at pH 8 in the presence of 0.1 and 0.4 M sodium perchlorate. The rate constant, $k_{obsd}°$, extrapolated to zero buffer concentration, was only 10–20% higher in the presence of the fourfold higher perchlorate ion concentration. The magnitude of this effect is consistent with a general salt effect. For example, a similar change in perchlorate concentration produces an approximately 10% acceleration in the pH-independent solvolysis of cyclopentadiene oxide,[18] which does not undergo nucleophilic attack by perchlorate ion. In contrast, an approximately threefold rate increase in the presence of 0.4 M, relative to 0.1 M, sodium perchlorate would have been predicted if nucleophilic attack by perchlorate ion at pH 8, with a rate constant linearly dependent on perchlorate ion concentration, had been responsible for the difference between the rates observed at pH 8 and pH 11–12.

**Scheme I**

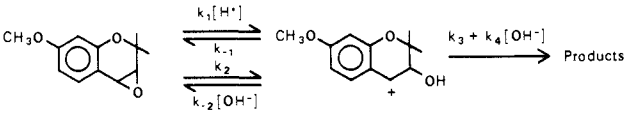


Further evidence for a change in rate-determining step for the solvolysis of **1** is provided by the observation that the pseudo-first-order rate constants exhibit a nonlinear dependence on buffer concentration (Figure 2). The curvature observed in these plots was observed both with the zwitterionic amino sulfonic acid buffers CHES and HEPES and with Tris. Buffer concentrations required for half maximal rate acceleration were comparable in magnitude (ca. 20 mM) for the three buffers. Curvature in rate vs buffer plots that results from complexation of a buffer species with a reactant should depend on the structure of the buffer; thus, it seems improbable that the nonlinear dependence of $k_{obsd}$ on buffer concentration for precocene oxide solvolysis in the case of three different buffers could be a result of such complexation. Analysis of the data by double-reciprocal plots of $1/(k_{obsd}-k_{obsd}°)$ vs $1/$[buffer] or by the use of a curve-fitting program, MLAB,[19] gave values for $k_\infty$, the limiting rate constant at high buffer concentration, that are dependent on hydronium ion activity (open symbols of Figure 1). The simplest explanation for this behavior is that the solvolysis reaction undergoes a change in rate-determining step from a buffer-catalyzed to a buffer-independent step as the concentration of the buffers is increased. Furthermore, the buffer-independent step ($k_\infty$) is first-order in hydronium ion over the pH range observed.

Solvolysis of **1** via a stepwise mechanism ($k_{st}$) such as that shown in Scheme I (or its kinetic equivalent; see below) can account for the observed pH–rate profile and the effect of buffers. At zero buffer concentration, steady-state treatment of the intermediate, CH$^+$, gives eq 1, where $K_1 = k_1/k_{-1}$.

$$k_{st}° = \frac{(k_3K_1a_{H^+} + k_4K_wK_1)(k_1a_{H^+} + k_2)}{k_3K_1a_{H^+} + k_4K_wK_1 + k_1a_H + k_2} \quad (1)$$

The following mechanism is consistent with the observed pH–rate profile. Suppose that $k_3 \gg k_{-1}$ (i.e., $k_3K_1 \gg k_1$) and $k_{-2} > k_4$ (i.e., $k_2 > k_4K_wK_1$). In regions A and B of Figure 1, $k_3$ is fast relative to $k_{-1}$ and $k_{-2}[OH^-]$, so that ring opening is rate-deter-

(13) Bruice, P. Y.; Bruice, T. C.; Dansette, P. M.; Selander, H. G.; Yagi, H.; Jerina, D. M. *J. Am. Chem. Soc.* **1976**, *98*, 2965–2973.
(14) Whalen, D. L.; Ross, A. M.; Dansette, P. M.; Jerina, D. M. *J. Am. Chem. Soc.* **1977**, *99*, 5672–5676.
(15) Whalen, D. L.; Ross, A. M. *J. Am. Chem. Soc.* **1976**, *98*, 7859–7861.
(16) Rogers, D. Z.; Bruice, T. C. *J. Am. Chem. Soc.* **1979**, *101*, 4713–4719.
(17) Becker, A. R.; Janusz, J. M.; Bruice, T. C. *J. Am. Chem. Soc.* **1979**, *101*, 5679–5687.
(18) Ross, A. M.; Pohl, T. M.; Piazza, K.; Thomas, M.; Fox, B.; Whalen, D. L. *J. Am. Chem. Soc.* **1982**, *104*, 1658–1665.
(19) Knott, G. D. *Comput. Programs Biomed.* **1979**, *10*, 271–280.

**Scheme II**

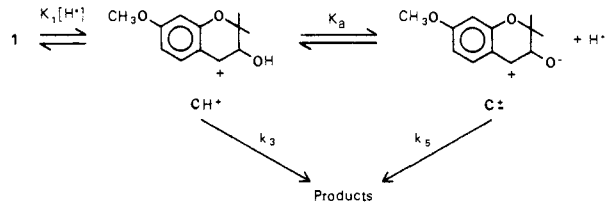


**Table I.** Rate Constants for Catalysis of the Solvolysis of **1** by Buffers[a]

| buffer | $pK_a$[b] | pH | $k_{HB}$,[c] $M^{-1}$ $s^{-1}$ |
|---|---|---|---|
| MES[d] | 6.17 | 6.53 | 152 |
| BES[d] | 7.08 | 7.09 | 38 |
| HEPES[e] | 7.49 | 7.97 | 51 |
| Tris[e] | 8.06 | 8.61, 9.00 | 29 |
| CHES[e] | 9.28 | 8.78, 9.28 | 4.4 ± 1.0 |

[a] At 25 °C in 1:9 dioxane–water, ionic strength 0.1 M ($NaClO_4$). [b] Estimated from measured pH values and the stoichiometry of the buffer solutions. [c] For the conjugate acid of the buffer. [d] Values of $k_{HB}$ were determined from the linear dependence of $k_{obsd}$ on buffer concentration (as the conjugate acid) at buffer concentrations between 0.5 and 2 mM. [e] Plots of $k_{obsd}$ vs buffer concentration for Tris, HEPES, and CHES buffers were nonlinear (cf. Figure 2). Values of $k_{HB}$ for these buffers were calculated as described in the Experimental Section.

mining. In region C, increasing hydroxide ion concentration results in $k_{-2}[OH^-]$ becoming larger than $k_3$, such that a change in rate-determining step from ring opening and its reverse to capture of the cation by water occurs. In region D, $k_4[OH^-]$ becomes appreciable, although still smaller than $k_{-2}[OH^-]$. Thus, the slowest kinetically significant step in this region is nucleophilic attack of hydroxide ion on the cation. When the appropriate inequalities are taken into consideration, eq 1 reduces to $k_{st}^\circ = k_1 a_{H^+}$ in region A and $k_{st}^\circ = k_2$ in region B. The pH-dependent rate constant observed in region C corresponds to $k_3K_1a_{H^+}$, whereas the predominant process contributing to the stepwise mechanism in region D corresponds to $k_4K_wK_1$.

The hydronium ion dependence of region C corresponds to specific acid catalysis and is a result of the fact that $CH^+$ and the transition state for its capture by water contain one more proton than the reactant epoxide. In region D, either the mechanism shown in Scheme I, involving $CH^+$ and a hydroxide ion, or a kinetically equivalent one involving a zwitterionic species ($C^\pm$; Scheme II) would result in mathematically identical rate expressions. In the latter case the rate constant for pH-independent product formation (region D) would be $k_5K_aK_1$.

The nonlinear plots (Figure 2) of rate constant vs buffer concentration in region B of the pH–rate profile are consistent with the interpretation that the buffers used catalyze the ring-opening step ($k_2$, $k_{HB}$) and the corresponding reverse processes, but not subsequent capture of the carbocation ($k_3a_{H^+}$). Steady-state treatment of the concentration of $CH^+$ gives eq 2 under conditions

$$k_{st} = \frac{(k_3K_1a_{H^+})(k_2 + k_{HB}[HB^+])}{k_3K_1a_{H^+} + k_2 + k_{HB}[HB^+]} = \frac{k_\infty(k_2 + k_{HB}[HB^+])}{k_\infty + k_2 + k_{HB}[HB^+])} \quad (2)$$

where $k_2 \gg k_1a_{H^+}$. In this equation, $k_{HB}$ is a second-order rate constant for general acid catalyzed ring opening by the conjugate acid of the buffer (Table I). At zero buffer concentration, $k_{st}^\circ$ is approximately equal to $k_2$, since (see above) $k_2$ is rate determining and $k_3K_1a_{H^+} > k_2$ in this pH region; at higher buffer concentration, $k_{st}$ approaches $k_\infty = k_3K_1a_{H^+}$, and thus the extrapolated values for $k_\infty$ (open symbols, Figure 1) are independent of buffer concentration and dependent on hydronium ion activity. These extrapolated values of $k_\infty$ gave an estimate of $k_3K_1 = 4 \times 10^7$ $M^{-1}$ $s^{-1}$, whereas curve fitting of eq 1 to observed pseudo-first-order rate constants at zero buffer concentration in region C of Figure 1 gave $k_3K_1 = 8 \times 10^7$ $M^{-1}$ $s^{-1}$. Use of an average value of $k_3K_1 = 6 \times 10^7$ $M^{-1}$ $s^{-1}$ provided an acceptable fit to all the data at both zero and high buffer concentrations (solid and broken lines of Figure 1). Considerable uncertainty in the value of $k_3K_1$ was expected for the following reasons: (i) $k_\infty$ is an *extrapolated* value and, furthermore, is derived from observed rates that are very rapid ($t_{1/2}$ = 2–3 s) at the highest buffer concentrations; (ii) the pH range over which $k_3K_1$ contributes to $k_{st}^\circ$ is very limited (about 1 pH unit, region C), and even in this range contributions of other processes ($k_2$, $k_4K_wK_1$) are significant.

**Table II.** Kinetic Constants for the Solvolysis of **1** at 25 °C in 1:9 Dioxane–Water, Ionic Strength 0.1 M ($NaClO_4$)[a]

| | | | |
|---|---|---|---|
| $k_r^H$, $s^{-1}$ | $2.6 \times 10^{-3}$ | $k_2$, $s^{-1}$ | $1.01 \times 10^{-2}$ |
| $k_r^D$, $s^{-1}$ | $6.5 \times 10^{-4}$ | $k_3K_1$, $M^{-1}$ $s^{-1}$ | $6.0 \times 10^7$ |
| $k_1$, $M^{-1}$ $s^{-1}$ | $1.16 \times 10^5$ | $k_4K_wK_1$, $s^{-1}$ | $9.6 \times 10^{-4}$ |

[a] For definitions, see Scheme IV and eq 6.

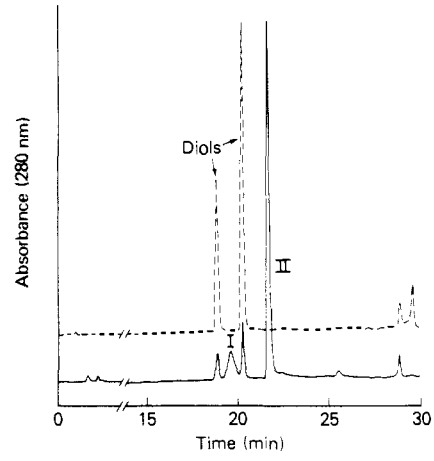


**Figure 3.** HPLC of products formed upon solvolysis of **1** in the presence (solid line) and absence (broken line) of 0.2 M acethydrazide at pH 8.5. The chromatography was carried out by using a Sota $C_{18}$ column, 4.6 × 250 mm, eluted at 1.5 mL/min with 25% methanol in 0.1 M ammonium acetate, pH 7.0, for 10 min, followed by a linear gradient to 80% methanol in 20 min. Peaks labeled I and II gave mass spectra corresponding to acethydrazide adducts of **1**.

The pH-dependent change in rate-determining step from buffer-catalyzed ring opening to uncatalyzed capture of $CH^+$ ($k_3$) in region C means that no buffer catalysis should be observed when $k_3$ is entirely rate-determining. Consideration of the rate constants shown in Table II indicates that $k_{-2}[OH^-]$ should be 1.7 times as large as $k_3$ at pH 10 (i.e., $k_2 = 1.7 \times K_1k_3a_{H^+}$), so that rate determination by $k_3$ is approached but not fully achieved in region C. At pH 10, 0.1 M CAPS buffer (70% as the conjugate acid) gave only a 30% rate increase relative to zero buffer, consistent with both a lower catalytic activity for this weakly acidic buffer and a greater contribution of the buffer-independent step to rate determination.

**Trapping of an Intermediate: Assignment of Rate-Determining Steps.** Although the observed dependence of the solvolysis rate on pH and buffer concentration is consistent with the mechanism of Schemes I or II with the rate-determining processes as described above, mathematically identical expressions would result from a mechanism in which the rate-determining steps were reversed, i.e., ring opening might be rate-determining in regions C and D and capture of the cation rate-determining in regions A and B of Figure 1. In this case, $k_{-1} \gg k_3$ and $k_4 > k_{-2}$. This ambiguity could be resolved if it were possible to trap the hypothetical intermediate with a nucleophile in a rapid step subsequent to rate-determining generation of the intermediate. Solvolysis of **1** at pH 8.5 and low buffer concentrations gives as the major products a pair of diols.[3] When this solvolysis was carried out in the presence of the nucleophile acethydrazide, $CH_3C(O)NHNH_2$, a large decrease in the amount of diol products ($t_R$ 18.9 and 20.3 min) was observed on HPLC, accompanied by the appearance of two new peaks ($t_R$ (minor) 19.6 min, (major) 21.7 min; see Figure 3) whose mass spectra corresponded to adducts derived from **1** and acethydrazide. Figure 4 illustrates the effect of increasing acethydrazide concentration on the recovery of diols

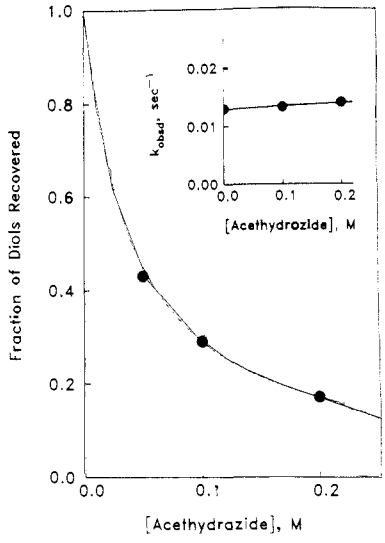


**Figure 4.** Effect of increasing concentrations of acethydrazide on the rate (inset) and products of solvolysis of **1** in 1 mM HEPES buffer at pH 8.5. The diol yield is expressed relative to that observed under the same conditions in the absence of acethydrazide.

and on the observed pseudo-first-order rate constants. Notably, in the presence of 0.2 M acethydrazide, the yield of diols is decreased by a factor of 5 relative to solvolysis in the absence of acethydrazide. Thus, by difference, 80% of the products formed in the presence of 0.2 M acethydrazide must result from adduct formation, yet there is virtually no effect of acethydrazide on the *rate constant* for reaction under these conditions (<10% increase, see inset of Figure 4). Reaction of the diol products with acethydrazide cannot account for our observations, since addition of 0.2 M acethydrazide *after completion* of the solvolysis reaction produced no significant decrease (<5%) in diol yield, relative to solvolysis in the absence of acethydrazide. Hence we conclude that, at pH 8.5, acethydrazide is trapping an intermediate in the solvolysis reaction, and that this *trapping occurs subsequent to the rate-determining step.* Thus, this observation provides both convincing evidence for the existence of an intermediate in diol formation from **1** and an unequivocal assignment of rate-determining steps for this process: *formation of the intermediate must be rate-determining in regions A and B* of the *pH-rate profile.*

**Products.** Futher insight into the nature of the kinetically significant processes in the solvolysis of **1** was obtained from analysis of the product distribution as a function of pH under the conditions of the kinetic measurements. Two experimental points are worthy of note.

(i) At neutral and basic pH values, the products of the reaction are pH-dependent and consist of the cis and trans diols[3] and a ketone that is presumably formed by a hydride shift from $C_3$ to $C_4$ of **1**, whereas at acidic pH values no ketone is detectable. The ketone is unstable at pH ≥10.5, and its extinction coefficient relative to the diols is unknown. Thus, HPLC quantitation of this product was most conveniently done by difference between the diol recovery at pH 5 and at the pH values of interest, with the assumption that no ketone is formed at the acidic pH. The validity of this method was verified by treatment of reaction mixtures with sodium borohydride after completion of the solvolysis reaction. The alcohol formed by reduction of the ketone should have an extinction coefficient similar to the diols, so that its direct quantitation relative to diols by integration of HPLC peaks is possible. At pH values of 9–10, product analyses by this method gave values for the fraction of ketone formed that agreed within 10% with values determined by difference, although at pH ≥10.5 instability of the ketone resulted in its incomplete recovery as the alcohol.

(ii) At pH values ≥10, where catalysis by low concentrations of buffers is negligible, product distribution was determined at a single buffer concentration (1–2 mM). At pH values 8–9, however, a substantial fraction of the observed rate, even at these

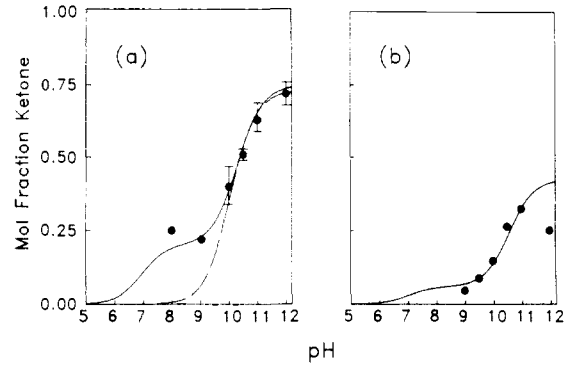


**Figure 5.** Effect of pH on the product distribution upon solvolysis of **1** (a) and **1** deuteriated at the 3-position (b). Points shown with error bars represent the average and range of three determinations. Where buffer dependence was observed, data were extrapolated to zero buffer concentration. The broken line of Figure 5a is a calculated curve for a mechanism in which ketone and diols are formed via a rapidly equilibrating pair of intermediates (see text). Solid lines are calculated on the basis of the mechanism of Scheme IV, with use of the kinetic constants given in Table II; for this mechanism, the dependence of the mole fraction of ketone formed ($f_k$) on pH is given by the equation $f_k = k_r/[k_r + (k_3K_1a_{H^+} + k_4K_wK_1)(k_1a_{H^+} + k_2)/(k_3K_1a_{H^+} + k_4K_wK_1 + k_1a_{H^+} + k_2)]$.

**Scheme III**

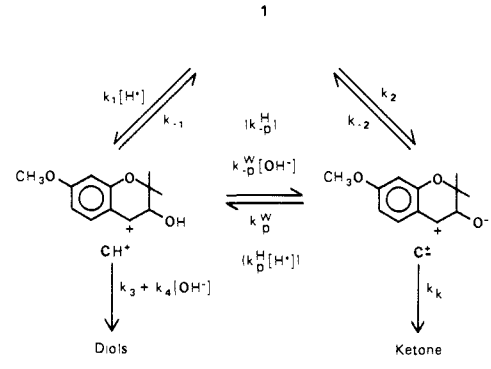


low buffer concentrations, results from buffer catalysis, and thus product distributions corresponding to $k_{obsd}^{\circ}$ (Figure 1) had to be obtained by extrapolation to zero buffer concentration. At relatively low buffer concentrations (where $k_{obsd}$ vs buffer concentration is linear), this extrapolation was most conveniently accomplished by plotting the reciprocal of the fraction ($f_k$) of ketone formed vs buffer concentration. The ordinate intercept of such a plot corresponds to the extrapolated value of $1/f_k$ at zero buffer.

Plots of the fraction of ketone product (extrapolated to zero buffer where necessary) as a function of pH are shown in Figure 5a. The diols were formed in a trans:cis ratio between 1.7:1 and 2:1 that remained essentially constant over the pH range 5–11. No ketone was detected at low pH. Above pH 7, the product profile shows two plateau regions, one at pH 8–9 (20% ketone) and one above pH 11 (75% ketone). An acceptable mechanism for product formation must account for this complexity.

A hypothetical mechanism for formation of ketone and diol products is shown in Scheme III. In this mechanism, diols arise from $CH^+$ whereas ketone is formed from the zwitterionic intermedate $C^{\pm}$. These intermediates are interconverted by proton transfer processes ($k_p$, $k_{-p}$). The predominant route for protonation of $C^{\pm}$ in the pH range 5–12 and in the absence of buffers should involve water as the proton donor ($k_p^w$), and the microscopic reverse, deprotonation of $CH^+$, should occur predominantly by hydroxide ion ($k_{-p}^w$) for the following reason. If a p$K$ of ca. 11–13 is assumed[20] for the hydroxyl group of $CH^+$, the pseudo-first-order

(20) The presence of a neighboring positive charge in geminal amino alcohols and related intermediates has been estimated to decrease the $pK_a$ of the hydroxyl group by ca. 4–5 units relative to the neutral alcohol. See, for example: Fox, J. P.; Jencks, W. P. *J. Am. Chem. Soc.* **1974**, *96*, 1436–1449. In the carbocation, charge delocalization could attenuate this effect to some extent.

**Scheme IV**

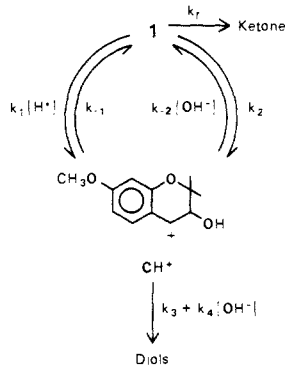


rate constant ($k_p^w$) for the protonation of C$^\pm$ by water[21] would be ca. $10^7$–$10^9$ s$^{-1}$, whereas for $a_{H^+} < 10^{-5}$ M, diffusion-controlled protonation by hydronium ion ($k_p^H a_{H^+}$) would have a pseudo-first-order rate constant $< 10^5$ s$^{-1}$, negligibly small compared with $k_p^w$. The simplest model for the mechanism shown in Scheme III involves the assumption that $CH^+$ and C$^\pm$ are interconverted much more rapidly than either species reverts to reactants or proceeds to products. This assumption of a rapidly equilibrating pair of ions is equivalent to the inequalities $k_{-p}^w[OH^-] \gg (k_{-1} + k_3 + k_4[OH^-])$ and $k_p^w \gg (k_{-2} + k_k)$.

A mechanism involving the assumptions described above cannot account for the observed product vs pH profile. Steady-state treatment of $CH^+$ and C$^\pm$, followed by elimination of terms on the basis of the above inequalities, gives eq 3a and 3b,

$$[CH^+] = \frac{(k_1[H^+] + k_2)[\mathbf{1}]}{K_e[OH^-](k_{-2} + k_k) + k_{-1} + k_3 + k_4[OH^-]} \quad (3a)$$

$$[C^\pm] = \frac{(k_1[H^+] + k_2)K_e[OH^-][\mathbf{1}]}{K_e[OH^-](k_{-2} + k_k) + k_{-1} + k_3 + k_4[OH^-]} \quad (3b)$$

where $K_e = k_{-p}^w/k_p^w$. Inspection of eq 3a and 3b indicates that $[C^\pm]/[CH^+] = K_e[OH^-]$. Furthermore, $K_e = K_a/K_w$, where $K_a$ is the dissociation constant of $CH^+$. Thus $[C^\pm]/[CH^+] = K_a/a_{H^+}$, as expected if complete equilibrium is established between these two species on a time scale that is rapid relative to the other bond making and breaking processes in the reaction scheme. The mole fraction of ketone at any pH is given by eq 4. Combination of

$$\text{mole fraction of ketone} = k_k[C^\pm]/(k_k[C^\pm] + (k_3 + k_4[OH^-])[CH^+]) \quad (4)$$

of the equilibrium equation with eq 4 gives eq 5, which corresponds

$$\text{mole fraction of ketone} = k_k K_a/(k_k K_a + k_3 a_{H^+} + k_4 K_w) \quad (5)$$

to a simple sigmoid curve with a *single inflection point* (ca. pH 10, cf. Figure 1) where the pH-dependent ($k_3 a_{H^+}$, region C) and pH-independent ($k_k K_a + k_4 K_w$, region D) processes for product formation are equal in rate. Thus, *this mechanism cannot account for the second inflection (20–0% ketone) that occurs below pH 7*, and we conclude that ketone and diols do not arise from two rapidly equilibrating ionic forms of an intermediate.

Two inflections in the product vs pH profile can be accounted for, however, if the ketone is formed via a single, pH-independent pathway that is *completely separate* from the stepwise mechanism proposed for diol formation, i.e. there is no interconversion between intermediates on the two pathways (Scheme IV). In such a scheme the first inflection point in the product vs pH curve corresponds to a change from exclusive diol formation ($k_1$) to the pH-independent region B where diol formation ($k_2$) is sufficiently slow that a separate, independent rearrangement pathway leading to ketone formation ($k_r$) becomes competititve. In this region, $k_2$ and $k_r$ both contribute to the rate and products, in a ratio of ca. 8:2. In regions A and B, ring opening is rate limiting for diol formation. As the pH is increased (region C), the rate of diol formation decreases, because of the change in rate-determining step as previously described, whereas the rate of ketone formation remains constant; thus, the proportion of ketone increases in this region. In region D, diol formation with $k_4$ rate determining is again pH-independent and occurs at a rate approximately one-third that for ketone formation.

Several mechanisms are consistent with discrete pathways for diol and ketone formation such that no "crossover" occurs between intermediates on the two pathways. For example, diol formation via $k_2$ may involve general acid catalysis by water to give $CH^+$, whereas ketone formation via $k_r$ may involve spontaneous ring opening to C$^\pm$. Although the exact timing, relative to C–O cleavage, of the proton transfer in the water-catalyzed reaction is not certain, rearrangement or capture of the intermediates $CH^+$ and C$^\pm$ must occur faster than the interconversion of these intermediates so that the initially formed intermediate, $CH^+$ or C$^\pm$, on each pathway is "committed" to that pathway, to give diols or ketone, respectively. Alternatively, the pathway for formation of the ketone may involve concerted C–O bond cleavage and hydride migration, with no intermediate, whereas diol formation requires $CH^+$ as an intermediate. It is likely that the hypothetical zwitterionic species C$^\pm$ is extremely unstable relative to **1** and that the energy barrier for collapse of C$^\pm$ to **1** is very small. This zwitterion may, in fact, be too unstable to exist at all, so that hydride migration (to give ketone) and/or proton transfer from water to the epoxide oxygen (to give $CH^+$, which yields diols) are constrained to occur simultaneously with C–O bond cleavage, via processes whose concerted nature is *enforced*[22] by the requirement for avoiding C$^\pm$.

We thus propose a mechanism (Scheme IV) for the reaction of **1** in aqueous solution in which diol and ketone formation are completely separate processes whose intermediates (if an intermediate exists in the case of ketone formation) do not interconvert on a kinetically significant time scale. Diol formation occurs via a pH-dependent, stepwise pathway ($k_{st}^\circ$) that involves $CH^+$ as a kinetically detectable intermediate, whereas ketone formation occurs exclusively via a pH-independent process ($k_r$) whose precise mechanistic details are unclear. The rate law for the overall reaction is given by eq 6; $k_{st}^\circ$, the rate for stepwise diol formation,

$$k_{obsd}^\circ = k_r + k_{st}^\circ = k_r + \frac{(k_3 K_1 a_{H^+} + k_4 K_w K_1)(k_1 a_{H^+} + k_2)}{k_3 K_1 a_{H^+} + k_4 K_w K_1 + k_1 a_{H^+} + k_2} \quad (6)$$

is from eq 1. Analysis of rate and product data as a function of pH gives the kinetic constants shown in Table II.

**Deuterium Isotope Effects.** Precocene oxide deuteriated at the 3-position exhibits *rate* isotope effects on solvolysis that are pH dependent, as expected if ketone formation is the only process that exhibits a significant (primary) deuterium isotope effect. Observed isotope effects on the measured pseudo-first-order rate constants at pH 7–11.4 are given in Table III. There is also a substantial isotope effect on the product distribution (Figure 5b). If the assumption is made that isotope effects on diol formation are

**Table III.** Deuterium Isotope Effects on the Rate Constants for Solvolysis of **1** at 25 °C, in 1:9 Dioxane–Water, Ionic Strength 0.1 M ($NaClO_4$)[a]

| pH | $k^H/k^D$ (obsd) | $k^H/k^D$ (calcd)[b] |
|---|---|---|
| 7.1 | 0.94 | 1.10 |
| 9.1 | 1.15 | 1.22 |
| 11.43 | 2.15 | 2.14 |

[a] In the absence of buffer catalysis or extrapolated to zero buffer concentration. [b] On the basis of eq 6 and the kinetic constants given in Table II. The assumption is made that $k^H/k^D = 1$ for all rate constants listed in Table II, except $k_r$, for which $k_r^H/k_r^D = 4$.

(21) The reverse of this reaction, deprotonation of $CH^+$ by hydroxide ion, should be diffusion-controlled, with a rate constant ($k_{-p}^w$) ca. $10^{10}$ M$^{-1}$ s$^{-1}$. Thus the forward rate constant ($k_p^w$) for protonation of C$^\pm$ by water would be $k_p^w = k_{-p}^w/K_e = 10^7$–$10^8$ s$^{-1}$, where $1/K_e$ is the equilibrium constant for protonation of C$^\pm$ by water, and is $10^{-2}$–$10^{-3}$ M on the basis of $K_w$ and the estimated p$K_a$ of $CH^+$.

(22) Jencks, W. P. *Acc. Chem. Res.* **1980**, *13*, 161–169.

negligible, then the kinetic isotope effect on *ketone formation* may be calculated from the *observed* isotope effects on the rate and products by using eq 7, where $f_k^H$ and $f_k^D$ are the fractions of

$$k_r^H/k_r^D = (k_{obsd}^H)(f_k^H)/(k_{obsd}^D)(f_k^D) = (k_{obsd}^H/k_{obsd}^D)(f_k^H/f_k^D) \quad (7)$$

ketone formed from the protio and deuterio substrates, respectively, as determined in separate experiments. The use of $f_k^H = 0.63$ and $f_k^D = 0.32$ at pH 11 (Figure 5) with $k_{obsd}^H/k_{obsd}^D = 2.15$ at pH 11.4 gives $k_r^H/k_r^D$ ca. 4 for ketone formation in region D of the pH–rate profile. Calculation of the expected kinetic isotope effects at lower pH values on the basis of eq 6 and the rate constants given in Table II gave values in satisfactory agreement with experimental data (Table III). An isotope effect of 4 is substantially larger than isotope effects previously observed for ketone formation in epoxide solvolysis reactions[23] and is in fact surprisingly large for a 1,2-hydride transfer reaction, for which deuterium isotope effects on the order of 2 are ordinarily observed.[24] The reason for the magnitude of this isotope effect is unclear. Although the value of 4 is only an approximation since the secondary isotope effects on diol formation are unknown and were assumed to be negligible,[25] there is obviously a large degree of zero-point energy loss of the hydrogen at $C_3$ in the transition state for ketone formation; i.e., this transition state does not resemble an unrearranged $C^{\pm}$ species, and substantial movement of this hydrogen must be occurring in the transition state.

## Summary and Conclusions

Epoxide solvolysis reactions differ from other solvolytic reactions (e.g., those of benzylic halides) in that the leaving group remains covalently attached to the molecule containing the cationic center after initial bond cleavage, thus facilitating return of the ionic intermediate to starting material. Although there is indirect evidence (from product stereochemistry and structure–reactivity correlations) for a carbocation intermediate in many solvolysis reactions of benzylic epoxides that give rise to highly stabilized carbocations, few studies have directly demonstrated the existence of such intermediates in epoxide solvolysis reactions. Furthermore, because the solvent is the nucleophile in these reactions, assignment of rate-determining step for these types of reactions is often not straightforward. Under acidic solvolysis conditions (pH <4), a chlorohydrin is formed from indene oxide in the presence of chloride ions, although at this pH chloride does not accelerate the reaction relative to perchlorate. This observation is most reasonably interpreted as a result of capture of a carbocation by chloride ion, in a step subsequent to rate-determining hydronium ion catalyzed ring opening.[15] Related effects of chloride ions at low pH on product distribution from tetrahydrophenanthrene[16] and tetrahydronaphthalene[17] oxides have been observed. Recently, the uncatalyzed solvolysis of *p*-methoxystyrene oxide was shown to be accompanied by deuterium scrambling between the trans and cis nonbenzylic positions of this epoxide under solvolytic conditions. A ring-opened intermediate that can undergo carbon–carbon bond rotation and reclosure to the epoxide faster than attack by solvent was proposed to account for this result.[26]

The present study provides direct kinetic evidence for the existence of an intermediate in an epoxide solvolysis reaction and, to our knowledge, represents the first definitive observation of such a reaction that undergoes a change in rate-determining step with changing pH and buffer concentrations. Trapping of the intermediate by an added nucleophile (0.05–0.2 M acethydrazide), at a rate that is competitive with water, demonstrates that the intermediate cation must be sufficiently stable to discriminate between nucleophiles. The stability of this intermediate is not surprising, in light of its resonance stabilization by oxygen substituents in both the ortho and para positions. The existence of a pH-dependent change in rate-determining step requires $k_{-2} > k_4$ and $k_3 \gg k_{-1}$ (Scheme IV). On the basis of the mechanism shown, this is reasonable, since proton abstraction ($k_{-2}$) from the hydroxyl group of $CH^+$ by hydroxide ion (with concomitant cyclization) may well be faster than C–O bond formation with hydroxide ion ($k_4$) to give diols. Since $k_{-2}$ is always greater than $k_4$, the change in rate-determining step occurs with increasing pH because increasing the hydroxide ion concentration favors the return of $CH^+$ to starting material ($k_{-2}$) relative to its capture by water ($k_3$). Surprisingly, however, this change in rate-determining step appears to be quite specific for **1**. We have examined a number of related compounds, including the epoxide of the desmethyl compound, 7-methoxy-2*H*-benzo[*b*]pyran, and have found no evidence for a change in rate-determining step. The reason for the unique behavior of **1** is at present unclear but may involve in part a retardation of the $k_4$ process by steric and/or solvation effects of the *gem*-dimethyl group.

## Experimental Section

**Materials.** Precocene I oxide was prepared, following the method of Jennings and Ottridge,[27] from precocene I (Aldrich) via the bromohydrin (formed by the use of *N*-bromoacetamide in aqueous THF). Dioxane used in kinetics experiments was distilled from sodium and stored frozen; deionized water was used in all kinetic experiments. Acethydrazide was recrystallized from ethanol. Buffer materials and inorganic compounds were commercially obtained and used without further purification.

7-Methoxy-2,2-dimethyl-2*H*-benzo[*b*]pyran-4(3*H*)-one (2.1 g), prepared by the method of Ohta and Bowers,[28] was deuteriated $\alpha$ to the carbonyl group by treatment at room temperature with a mixture of deuteriomethanol/deuterium oxide containing a trace of sodium deuteroxide for a period of 16 h. The solvent was removed by evaporation, and the procedure repeated for three additional cycles, upon which time the mixture was neutralized with deuteriosulfuric acid. Evaporation of solvent and recrystallization of the residue from hexane gave colorless plates (1.7 g, 81%) of ketone. Mass spectral analysis showed the compound to contain ca. 96% dideuterio, ca. 2% monodeuterio, and ca. 2% diprotio ketone.

7-Methoxy-2,2-dimethyl-2*H*-benzo[*b*]pyran-4(3*H*)-one-3-$^2H$ was reduced with lithium aluminum hydride in ether at room temperature in an argon atmosphere. The reaction mixture was quenched with deuterium oxide, extracted with ether, washed with sodium chloride solution, and dried over sodium sulfate. Removal of the solvent left the product 3,4-dihydro-4-hydroxy-7-methoxy-2,2-dimethyl-2*H*-benzo[*b*]pyran-3-$^2H$ as a colorless oil (290 mg, 97%).

3,4-Dihydro-4-hydroxy-7-methoxy-2,2-dimethyl-2*H*-benzo[*b*]pyran-3-$^2H$ (290 mg) in dioxane containing a trace of pyridine was refluxed with trifluoroacetic anhydride (446 mg) for 1 h. The reaction mixture was poured into water and extracted with ether. Workup provided precocene I-3-$^2H$ (150 mg, 57%) as a volatile liquid.

Precocene I-3-$^2H$ was converted to its bromohydrin as described. The bromohydrin was purified by HPLC on a Du Pont Zorbax SIL column, 9.4 × 250 mm, eluted with 20% ether in petroleum ether; $k' = 4$. Mass spectral analysis of the bromohydrin indicated 97% incorporation of deuterium. Precocene I-3-$^2H$ oxide was prepared by treatment of the bromohydrin with sodium hydride in THF as described by Jennings and Ottridge.[27]

**Kinetics.** All rates were determined at 25 °C in 1:9 (v/v) dioxane–water. Ionic strength was maintained at 0.1 M by the addition of sodium perchlorate. The pH was maintained by the use of Tris, BES (*N*,*N*-bis(2-hydroxyethyl)-2-aminoethanesulfonic acid), MES (2-*N*-morpholinoethanesulfonic acid), HEPES (4-(2-hydroxyethyl)-1-piperazineethanesulfonic acid), CHES (2-(cyclohexylamino)ethanesulfonic acid) or CAPS (3-(cyclohexylamino)-1-propanesulfonic acid) buffers. For buffer catalysis experiments with HEPES, Tris, and CHES, a range of total buffer concentrations between 1 and 100 mM was generally used. Because of strong buffer catalysis at pH values <10, as well as the nonlinear dependence of the rate on buffer concentration at high concentrations of these buffers (cf. Figure 2), separate experiments were used to obtain accurate values of $k_{obsd}^0$ as a function of pH. In these experiments, rate constants were determined at each pH value of interest at four buffer concentrations between 0.5 and 2 mM (BES, MES) and

(23) Sayer, J. M.; Yagi, H.; Silverton, J. V.; Friedman, S. L.; Whalen, D. L.; Jerina, D. M. *J. Am. Chem. Soc.* **1982**, *104*, 1972–1978. Gillilan, R. E.; Pohl, T. M.; Whalen, D. L. *Ibid.* **1982**, *104*, 4482–4484.

(24) Collins, C. J.; Rainey, W. T.; Smith, W. B.; Kaye, I. A. *J. Am. Chem. Soc.* **1959**, *81*, 460–466. More O'Ferrall, R. A. *J. Chem. Soc. B* **1970**, 785–790 and references therein.

(25) Hanzlik, R. P.; Westkaemper, R. B. *J. Am. Chem. Soc.* **1980**, *102*, 2464–2467.

(26) Ukachukwu, V. C.; Blumenstein, J. J.; Whalen, D. L. *J. Am. Chem. Soc.* **1986**, *108*, 5039–5040.

(27) Jennings, R. C.; Ottridge, A. P. *J. Chem. Soc., Chem. Comm.* **1979**, 920–921.

(28) Ohta, T.; Bowers, W. S. *Chem. Pharm. Bull.* **1977**, *25*, 2788–2789.

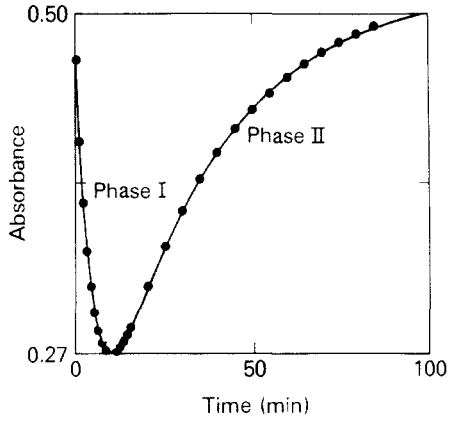


**Figure 6.** Observed absorbance changes at 239 nm upon solvolysis of **1** at pH 11.2. Analysis of the data by using eq 8 gave a rate constant of $3.7 \times 10^{-3}$ $s^{-1}$ for the solvolysis reaction (Phase I). The nature of the secondary process (Phase II) is unknown; presumably it involves a slow reaction of the 3-ketone produced, which was observed to be unstable at high pH.

between I and 4 mM (Tris), or at two to three buffer concentrations between 0.25 and 1 mM (HEPES, CHES). The observed pseudo-first-order rate constants were then extrapolated to zero buffer concentration. At pH values >10, the rate is insensitive to low concentrations of buffers. Thus, rate constants, $k_{obsd}^{\circ}$, at pH values ≥10.5 were determined at a single buffer concentration (1 mM), since extrapolation was unnecessary.

Reactions were initiated by the addition of 2–3 μL of a precocene oxide solution in THF or dioxane to 3 mL of buffer solution, and the rate of disappearance of the oxide was measured at 239 nm; sufficient precocene oxide was used to give a total change of ca. 0.3–0.5 absorbance units. At pH values ≥10.5, stable endpoints could not be obtained at 239 nm due to a secondary increase in absorbance subsequent to the initial relatively rapid reaction. This slow increase had a half-life ca. 10–40 times longer than that for the initial absorbance decrease due to the solvolysis reaction. At the highest pH value measured (ca. 11.5), this difficulty was most conveniently avoided by following the reaction at 288 nm, an isosbestic point for the slow process. Since this isosbestic point appeared to be pH-dependent, corrections for unstable endpoints at lower pH values were made as follows: the absorbance change at 239 nm was followed for 30–250 half-lives of the initial reaction. With use of the program MLAB,[19] the observed absorbance changes were then fit to a rate equation for sequential first-order reactions (eq 8), where $k_1$ is the rate

$$A_{obsd} = A_0e^{-k_1t} + [A_0\epsilon_B k_1/(k_2 - k_1)](e^{-k_1t} - e^{-k_2t}) + A_0\epsilon_C[1 + 1/(k_1 - k_2)](k_2e^{-k_1t} - k_1e^{-k_2t}) \quad (8)$$

constant for solvolysis (the initial phase of reaction), $k_2$ is the rate constant for the secondary reaction ("endpoint change"), and $\epsilon_B$ and $\epsilon_C$ are *relative* extinction coefficients for the primary and secondary products, respectively. A typical plot of the time course of the absorbance changes observed at pH 11.2 is shown in Figure 6.

**Product Determinations.** Products of the solvolysis of **1** at ambient temperature were determined in reaction mixtures containing sodium perchlorate and dioxane concentrations identical with those used in the kinetic studies. At pH values > 9.05, a single buffer concentration (1 or 2 mM) was used, whereas at lower pH values (7–9) products were determined at buffer concentrations between 0.25 and 5 mM, and the results were extrapolated to zero buffer concentration by plotting $1/f_k$ vs buffer concentration, where $f_k$ is the fraction of ketone product. Products were analyzed by HPLC on a Vydac $C_{18}$ column, 4.6 × 250 mm, eluted with 30% methanol in water for 5 min followed by a linear gradient to 90% methanol in water over 20 min. at a flow rate of 1.5 mL/min. Under these conditions the cis and trans diols derived from solvolysis of **1** are eluted at 4.6 and 5.2 min, respectively. Uniformity of injections was ensured by the use of a Perkin-Elmer autosampler. Diols were quantitated by integration of the peaks monitored at 280 nm, and ketone, when formed, was determined by difference between the diols recovered at a given pH and diols formed at pH 5 (1 mM MES buffer), where no ketone product was observed and 100% conversion of the epoxide to the diols was assumed. An identical recovery of diols was observed in the absence of any buffer at pH 3. In a separate experiment, reaction mixtures were quenched with acid after ca. 5 half-lives and subjected to reduction with sodium borohydride, followed by HPLC as described. Under these conditions, a new peak, $t_R$ 8.6 min, which was ascribed to the 3-hydroxy compound, was observed: mass spectrum (CI, $NH_3$), $m/z$ 208 $(M + 1)^+$. Since this product, derived from reduction of the ketone, should have an extinction coefficient similar to that of the diols, direct quantitation of diols and ketone was possible in these experiments. At pH values < 10.5, acceptable agreement (±10%) was observed between the fractional yields of ketone determined as the 3-hydroxy derivative and those estimated by difference; however, at higher pH values, instability of the ketone during the time required for solvolysis resulted in its incomplete recovery as the borohydride reduction product.

**Determination of Rate Constants from Kinetic and Product Data.** The value of $k_1$, and trial values for $k_2$, $k_3K_1$, and $k_4K_wK_1$ were estimated by curve fitting of eq 1 to values of $k_{obsd}^{\circ}$ (extrapolated to zero buffer concentration) as a function of pH by using the computer program MLAB.[19] In this initial calculation, $k_{st}^{\circ}$ (eq 1) was assumed to be equal to $k_{obsd}^{\circ}$. The rate constant, $k_3K_1$, was also determined from the linear pH dependence of $k_\infty$ (eq 2), and an average value of $6 \times 10^7$ $M^{-1}$ $s^1$ was used for $k_3K_1$ in subsequent calculations. For determination of $k_r$, the rate constant for ketone formation, the product vs pH data of Figure 5a were combined with rate constants for total reaction estimated from the pH–rate profile, such that $(k_{obsd}^{\circ})(f_k) = k_r$, where $f_k$ = fraction of ketone. The average value of $k_r$ determined from the six pH points shown in Figure 5a was substituted into eq 6. Repetition of the curve-fitting program provided corrected values for $k_2$ and $k_4K_wK_1$.

Rate constants for buffer catalysis (Table I) were calculated from nonlinear plots of $k_{obsd}$ vs buffer concentration by curve fitting of eq 2, after correcting the observed rate constants for the contribution of concerted ketone formation by using the relationship $k_{st} = k_{obsd} - k_r$.

**Trapping Experiments with Acethydrazide.** Solvolysis of **1** was carried out, under the conditions described above for kinetic studies, in the presence of 1 mM HEPES buffer (pH 8.5) and 0.05–0.20 M acethydrazide. Reaction rates in the presence of acethydrazide were followed spectrophotometrically at 276 nm because of the interfering absorbance of acethydrazide at 239 nm.

Products of the reaction in the presence of acethydrazide were analyzed by HPLC (cf. Figure 3). Diol recovery was quantitated by the difference between the total area corresponding to diols in the presence and absence of acethydrazide at the same pH. Two new peaks, which appeared in the chromatograms of reaction mixture containing acethydrazide, had $t_R$ 19.6 min (minor) and 21.7 min (major): mass spectrum (DCI, $NH_3$) (relative intensity) for the minor product: $m/z$ 298 $(M + NH_4)^+$ (4), 281 $(M + H)^+$ (18), 207 $(M - [NHNHCOCH_3])^+$ (100). For the major product: $m/z$ 298 (2), 281 (5), 207 (100). To verify that these adducts were formed from an *intermediate*, rather than from a product of the reaction, a total of 0.2 M acethydrazide was added to a reaction mixture after completion of the solvolysis at pH 8.5, and HPLC of the mixture was performed.